The Influence of Self-User Shadowing in the Intra-Metro Communication Scenario at 28 GHz

Yuxuan Xu*, Danping He†‡, Haofan Yi†‡, Ke Guan†‡, Mikko Heino§, Marko Sonkki¶
*School of Electronic and Information Engineering, Beijing Jiaotong University, 100044, Beijing, China
†State Key Laboratory of Rail Traffic Control and Safety, Beijing Jiaotong University, 100044, Beijing, China
‡Beijing Engineering Research Center of High-speed Railway Broadband Mobile Communications, 100044, Beijing, China
§Department of Electronics and Nanoengineering, Aalto University, Finland
¶Centre for Wireless Communication (CWC), University of Oulu, Oulu, Finland
E-mail: hedanping@bjtu.edu.cn, Corresponding author: Danping He

***Abstract*—Nowadays metro plays an important role in people's daily life. It is significant to realize a high-data-rate wireless connectivity in metro carriages. In this paper, the intra-metro channels with the consideration of self-user shadowing at 28 GHz are characterized by ray-tracing (RT) simulation. The three-dimensional metro model is reconstructed according to the actual size of Madrid Metro. Based on the RT simulation results, totally six cases (three transmitter deployments, with and without self-user shadowing) are characterized in terms of angular spreads, received power, root-mean-square (RMS) delay spread. Once the user shadows the channel, the received power will be approximately 15-25 dB less than that of unoccupied. Compared with the parameters of angular spreads and RMS delay spread without shadowing, the wireless link is established by Non-LOS due to the self-user shadowing effect. These results provide valuable insights into the system design and evaluation for wireless communications inside the metro scenario.**

***Index Terms*—Channel characterization, metro, ray-tracing, self-user shadowing, 28 GHz.**

I. Introduction

In the vision of "SmartMetro", infrastructure, metros, riders will be increasingly interconnected. Correspondingly, a high-data-rate wireless connectivity with up to dozens of GHz bandwidth will be required to provide various bandwidth intensive applications, such as high definition (HD) video, real-time HD conference call and on-board real-time high-data rate connectivity [1], [2]. Millimeter-wave (mmWave) bands are an ideal spectrum candidate for fifth-generation communications systems (5G). It could be exploited to increase the capacity and enable the users to experience several Gbps data rates [3]–[5]. One of the practical issues in cellular mobile radios operating at higher frequency bands is its coverage. Higher radio frequencies typically have smaller service coverage compared to lower frequency radio, particularly in non-line-of-sight conditions in light of greater signal losses in diffraction and penetration of radio wave propagation.

At mmWaves, the far-field shadowing due to different objects e.g. humans, has been noted to be significant. The shadowing of a human can be modelled with simple models, e.g. with a cylinder [6]. Full-wave simulation of the whole human becomes a difficult problem. In [7], a human shadowing model was presented at 28 GHz using finite difference time-domain (FDTD) simulation method with human shadowing measurements. In [8], a detailed surface-based human shadowing model usable with an integral equation (IE) solver was presented to reduce the simulation time compared to FDTD method significantly. In the existing research, most of the efforts were made on various metro environments. Power attenuation, shadowing, Rician K-factor, channel dispersions, etc., have been investigated in tunnels [9], [10]. However, due to totally incomparable environments, the mentioned studies can be hardly transferred to the intra-metro channel. Besides, due to particular geometry and the effect of self-user shadowing in the metro, the intra-metro channel is even different from other intra-vehicle environments, e.g., intra-plane [11], intra-ship [12], and intra-container [13]. Thus, it is of importance to characterize the intra-metro channels considering the self-user shadowing effects through simulation in realistic metro.

In this paper, we characterize the intra-metro channel considering the self-user shadowing effects at the 28 GHz band comprehensively with the following contributions: we reconstruct the intra-metro scenario and conduct the simulations using the ray-tracing (RT) simulator with different positions of transmitter (Tx) and two kind of receiving antennas. Based on the RT simulation results, the channel of intra-metro scenario considering the self-user shadowing is characterized in terms of received power, root-mean-square (RMS) delay spread, azimuth angular spread of departure (ASD), azimuth angular spread of arrival (ASA), elevation angular spread of departure (ESD), and elevation angular spread of arrival (ESA), respectively. Through the analysis of these parameters, we evaluate the influence of self-user shadowing. These parameters will provide the fundamentals for designing wireless communications systems in a similar scenario.

The rest of this paper is organized as follows: Section II describes the RT simulation in the metro model with six cases (three Tx deployments with two kinds of receiving antennas). Section III shows the result of simulation and compares channel characteristics between different cases. Section IV concludes this paper.

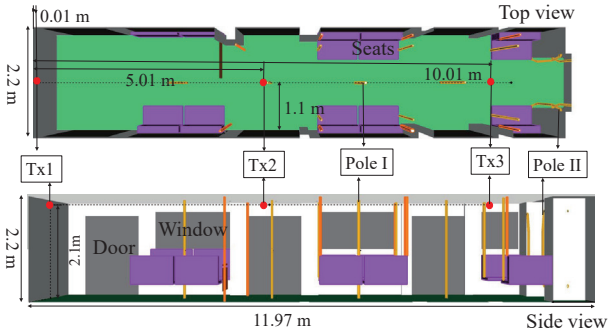

Fig. 1. Top and side view of the metro carriage model.

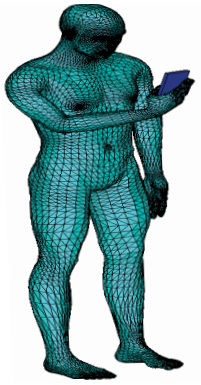

Fig. 2. One-hand grip where the phone is oriented vertically [8].

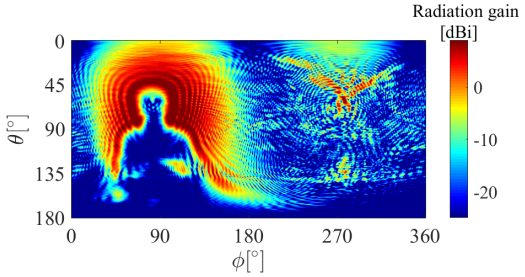

Fig. 3. 3D pattern of the antenna with self-user shadowing.

II. Communication Environment and Configuration Setups

The RT simulator employed in this study is self-developed by Beijing Jiaotong University and Technische Universität Braunschweig. It is composed of a vehicle-to-vehicle RT simulator [14] and an ultra-wideband Terahertz RT simulator [15]. It has been successfully applied in different works [16] [17]. Recently, this RT simulator is extended to a high-performance computing cloud-based platform. More details of this platform can be found in [18] as well as the website http://raytracer.cloud.

In this section, we utilize the RT simulator with the three-dimensional (3D) model according to the actual size of Madrid Metro. The width, length and height are 2.2 m, 11.97 m, and 2.2 m, respectively. The main visible objects are the train body, the seats, the windows, the poles/handrails, etc. There are three Tx deployments, where each deployment has only one Tx. Each Tx is 2.1 m high and 1.1 m away from the carriage wall. As shown in Fig. 1, the first deployment is located away from the head of carriage 0.01 m with the ID of Tx1. The second deployment is located away from the head of carriage 5.01 m with the ID of Tx2. The third deployment is located away from the head of carriage 10.01 m with the ID of Tx3. In this study, we pay more attention to the influence of self-user shadowing on the channel, so the Tx is set as an omnidirectional antenna to find the channel characteristics in the metro.

In order to compare the influence of self-user shadowing on the channel, two types of antennas are provided. One is a mobile phone antenna shadowed by the user, and the other is an omnidirectional antenna. The simulation result of the first kind of antenna in [8] is the most typical case when a user is holding the mobile phone in a data browsing stance with one hand in Fig. 2. The mobile phone antenna is pointing directly towards the user, leading to the blockage of the radiated or received field at the antenna due to a body in front. The phone is placed symmetrically with respect to the center of the head and the mobile phone is tilted 20° away from the z-axis. 3D pattern of the antenna gain with shadowing is shown in Fig. 3. The dataset with the standing human can be find in [19].

Considering the random direction of the person in the carriage, we set the direction of the receiving antenna to be random, but in order to compare the channel characteristics of different deployments, we have the same group of random data applied to these in comparison to the same situation without self-user shadowing. In the simulation, the receiver (Rx) is traversing the compartment. Rx is set to be 1.5 m high (which emulates the heights of the mobile phones, when the user is standing) and located through the whole metro with 0.2 m×0.2 m spatial resolution. The propagation mechanisms are line-of-sight (LOS), up to second-order reflection, and scattering. Details of the simulation setups are given in Table I. The calibrated electromagnetic (EM) parameters from our previous work [5] are summarized in Table II. $\epsilon_r^{'}$ is the real part of permittivity. tanδ is the loss tangent. S is the scattering gain, and α is the effective roughness in the directive scattering model [20].

TABLE I
SIMULATION SETUPS

Scenario	Intra-metro
Antenna type	Omni-directive Mobile phone patch antenna at 28 GHz with human shadowing
Polarization	vertical-vertical polarization
Receiver height	1.5 m
System bandwidth	1 GHz
Frequency range	27.5-28.5 GHz
Frequency points	100
Propagation	LOS, scattering, and reflection (up to 2nd order)

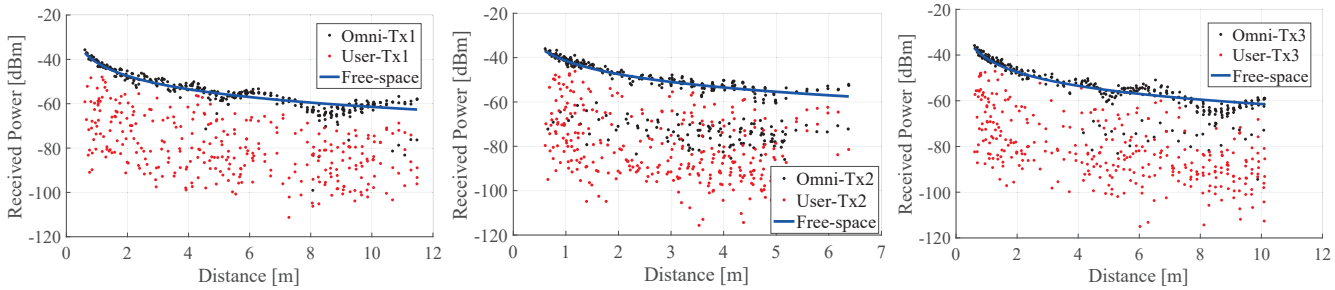

(a) Received Power-Tx1 (b) Received Power-Tx2 (c) Received Power-Tx3

Fig. 4. Received power.

TABLE II
EM PARAMETERS OF MATERIALS

Object Name	Calibrated parameters			
	ϵ_r'	tanδ	S	α
Side walls	1.0285	5.60e-2	7.30e-3	10
Seats	1.0146	6.20e-2	4.40e-3	31
Doors, windows	1.0000	1.40e-1	1.30e-3	43
Floor	6.9900	5.00e-3	1.86e-4	30
Ceiling	1.0000	1.00e7	1.30e-4	62
Junction	1.0000	1.00e7	9.10e-3	6
Pole I	1.0077	5.67e-1	1.30e-3	62
Pole II	1.0171	4.15e-1	1.30e-3	62

III. RESULT ANALYSIS

Based on the RT simulation results, we make comperhensive characterization for the intra-metro channels at the 28 GHz with six cases. The channel characteristics include received power, RMS delay spread, and angular spreads.

A. Received Power

The values of received power are shown in Fig. 4a, Fig. 4b, and Fig. 4c, respectively. When Tx is at both ends of the carriage, there are not as many multipath components as Tx is in the middle of the carriage, so it is more consistent with the free space propagation model when there is no shadowing from the user. As Tx is rich in multipath components in the middle of the carriage, multipath coherent superposition appears, resulting in the fluctuation of the received power. Generally, once the user shadow the channel, the Rx receiving power will be approximately 15-25 dB less than that of unshadowed. Hence, the high-gain antennas at both sides of Tx and Rx are required to build the effective wireless link at mmWave frequence band.

B. RMS delay spread

The values of RMS delay spread are shown in Fig. 5. The results are compared in different Tx positions. When Tx is in the middle of the carriage, RMS delay spread is significantly larger than the Tx at both ends of the carriage. This is because there are more effective multipath components between Tx and Rx when Tx is located in the middle of the carriage.

Generally, the median value of RMS delay spread is larger when the self-user shadowing is under consideration for each

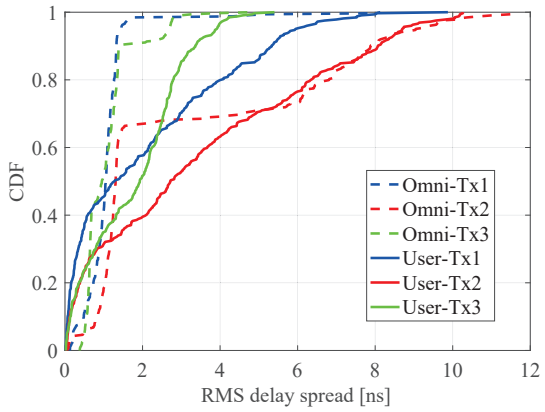

Fig. 5. RMS delay spread.

Tx position. This is mainly because the LOS path energy is blocked due to the self-user shadowing. The connection is not build only in expection of the LOS paths, but through the NLOS paths through reflection and scattering.

C. Angular Spreads

The four angular spreads (ASD, ASA, ESD, and ESA) are calculated through the same approach of 3GPP standards [21]:

$$\sigma_{AS} = \sqrt{\frac{\sum_{n=1}^{N} (\theta_{n,\mu})^2 \cdot P_n}{\sum_{n=1}^{N} P_n}}. \tag{1}$$

where σ_{AS} denotes the angular spread, P_n denotes the power of the n-th multipath, $\theta_{n,\mu}$ is defined by

$$\theta_{n,\mu} = \text{mod}\,(\theta_n - \mu_\theta + \pi, 2\pi) - \pi. \tag{2}$$

where θ_n is azimuth angle of arrival (AoA), azimuth angle of departure (AoD), elevation angle of arrival (EoA), elevation angle of departure (EoD) of the n-th multipath and μ_n is calculated by

$$\mu_\theta = \frac{\sum_{n=1}^{N} \theta_n \cdot P_n}{\sum_{n=1}^{N} P_n}. \tag{3}$$

The values of ASD are shown in Fig. 6a. Since the deployment of Tx3 is not close to the wall but with a distance

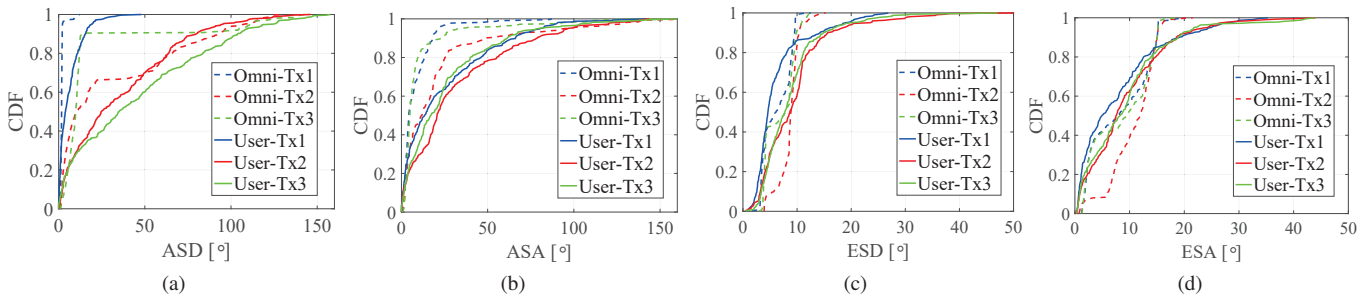

Fig. 6. Angular spreads.

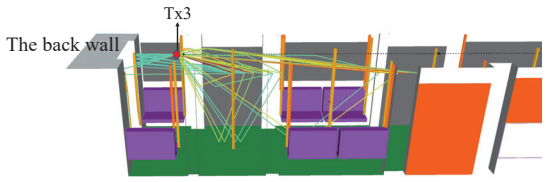

Fig. 7. One snapshot of RT simulation.

of 1.9 m, the multipaths reflected from the back wall can expend the values of ASD as shown in Fig. 7 as an example. This is the reason why the median value of ASD of Tx3 is larger than it of Tx1. Under the same Tx position, when the channel is shadowed by the user, the median values of ASD is larger than the unoccupied one. The main reason is that the Tx cannot establish a connection with Rx only through the LOS paths because of the self-user shadowing. It builds effective connections with Rx through the NLOS paths in other directions mostly. In the absence of self-user shadowing, the channel between the Tx and the Rx is primarily the LOS path. Hence, when Rx is an omnidirectional antenna, the ASD is concentrated in a small angle.

The values of ASA are shown in Fig. 6b. When Tx is in the middle of the carriage, the median value of ASA is larger than the Tx at the two ends of the carriage. The reason is that the Tx forms more effective multipath components with Rx in the middle of the carriage. Generally, when the user shadows the channel, the median value of ASA is obviously larger than the unoccupied one for each Tx position. Some LOS paths cannot establish an effective connection due to the random direction of the person in the metro. It is necessary to establish connections with Rx through the Non-LOS (NLOS) paths, so the median value of ASA is larger.

The values of ESD, ESA are shown in Fig. 6c and Fig. 6d, respectively. Since the Tx is at the ceiling of the carriage, the difference between the different positions of the Tx and the difference between the presence or absence of the self-user shadowing is not obvious for ESA and ESD. Besides, there is no significant difference between departure and arrival in terms of elevation angular spread.

Overall, the azimuth angular spread is significantly larger than the elevation angular spread for both departure and arrival. It is indicated that the multipath components in the carriage are more dispersed than the elevation plane in the azimuth plane.

IV. Conclusion

In this paper, the intra-metro channels with the consideration of self-user shadowing at 28 GHz are characterized by RT simulation. The 3D metro model is reconstructed according to the actual size of Madrid Metro. Totally six cases (three transmitter deployments, with and without self-user shadowing) are characterized. Generally, once the user shadows the channel, the receiver receiving power will be approximately 15-25 dB less than that of unshadowed. Hence, the high-gain antennas at both sides of Tx and Rx are required to build the effective wireless link at mmWave frequence band. Compared with the two parameters of ASD and RMS delay spread without shadowing, the wireless link is established by NLOS due to the self-user shadowing effect. The results show that besides the LOS path, the reflection and scattering also have a significant influence on the channel.

Acknowledgment

This work is supported by NSFC under Grant 61901029, 61771036, and 61911530771, Academy of Finland project under grant 323857.

References

[1] R. He, Z. Zhong, B. Ai, K. Guan, B. Chen, J. I. Aionso, and C. Briso, "Propagation channel measurements and analysis at 2.4 GHz in subway tunnels," *IET Microwaves, Antennas Propagation*, vol. 7, no. 11, pp. 934–941, August 2013.

[2] H. Jenq-Neng and W. Yonggang, "Next generation mobile video networking," *ZTE Communications*, vol. 16, no. 3, pp. 5–6, 2018.

[3] W. Roh, J. Seol, J. Park, B. Lee, J. Lee, Y. Kim, J. Cho, K. Cheun, and F. Aryanfar, "Millimeter-wave beamforming as an enabling technology for 5G cellular communications: theoretical feasibility and prototype results," *IEEE Communications Magazine*, vol. 52, no. 2, pp. 106–113, February 2014.

[4] J. Wells, "Faster than fiber: The future of multi-G/s wireless," *IEEE Microwave Magazine*, vol. 10, no. 3, pp. 104–112, May 2009.

[5] C. Zheng, Z. Xu, D. He, K. Guan, B. Ai, and J. M. García-Loygorri, "Millimeter wave channel measurement based ray-tracing calibration and analysis in metro."

[6] C. Gustafson and F. Tufvesson, "Characterization of 60 GHz shadowing by human bodies and simple phantoms," in *2012 6th European Conference on Antennas and Propagation (EUCAP)*, March 2012, pp. 473–477.

[7] I. Syrytsin, S. Zhang, and G. F. Pedersen, "User impact on phased and switch diversity arrays in 5G mobile terminals," *IEEE Access*, vol. 6, pp. 1616–1623, 2018.

[8] M. Heino, C. Icheln, and K. Haneda, "Self-user shadowing effects of millimeter-wave mobile phone antennas in a browsing mode," in *2019 13th European Conference on Antennas and Propagation (EuCAP)*, March 2019, pp. 1–5.

[9] M. M. Rana and A. S. Mohan, "Segmented-locally-one-dimensional-FDTD method for EM propagation inside large complex tunnel environments," *IEEE Transactions on Magnetics*, vol. 48, no. 2, pp. 223–226, Feb 2012.

[10] R. Lanzo, M. Petra, and L. Stola, "Ray tracing model for propagation channel estimation in tunnels and parameters tuning with measurements," in *The 8th European Conference on Antennas and Propagation (EuCAP 2014)*, April 2014, pp. 1785–1788.

[11] H. Saghir, C. Nerguizian, J. J. Laurin, and F. Moupfouma, "In-cabin wideband channel characterization for WAIC systems," *IEEE Transactions on Aerospace and Electronic Systems*, vol. 50, no. 1, pp. 516–529, January 2014.

[12] X. H. Mao and Y. H. Lee, "UHF propagation along a cargo hold on board a merchant ship," *IEEE Transactions on Wireless Communications*, vol. 12, no. 1, pp. 22–30, January 2013.

[13] E. Tanghe, W. Joseph, P. Ruckebusch, L. Martens, and I. Moerman, "Intra-, inter-, and extra-container path loss for shipping container monitoring systems," *IEEE Antennas and Wireless Propagation Letters*, vol. 11, pp. 889–892, 2012.

[14] K. Guan, Z. Zhong, B. Ai, and T. Kürner, "Deterministic propagation modeling for the realistic high-speed railway environment," in *2013 IEEE 77th Vehicular Technology Conference (VTC Spring)*, Dresden, Jun. 2013, pp. 1–5.

[15] S. Priebe and T. Kürner, "Stochastic modeling of THz indoor radio channels," *IEEE Transactions on Wireless Communications*, vol. 12, no. 9, pp. 4445–4455, September 2013.

[16] K. Guan, B. Ai, B. Peng, D. He, G. Li, J. Yang, Z. Zhong, and T. Kürner, "Towards realistic high-speed train channels at 5G Millimeter-Wave band—part I: Paradigm, significance analysis, and scenario reconstruction," *IEEE Transactions on Vehicular Technology*, vol. 67, no. 10, pp. 9112–9128, Oct 2018.

[17] ——, "Towards realistic high-speed train channels at 5G millimeter-wave band—part II: Case study for paradigm implementation," *IEEE Transactions on Vehicular Technology*, vol. 67, no. 10, pp. 9129–9144, Oct 2018.

[18] D. He, B. Ai, K. Guan, L. Wang, Z. Zhong, and T. Kürner, "The design and applications of high-performance ray-tracing simulation platform for 5G and beyond wireless communications: A tutorial," *IEEE Communications Surveys Tutorials*, vol. 21, no. 1, pp. 10–27, Firstquarter 2019.

[19] M. Heino, C. Icheln, and K. Haneda, "Simulated self-user shadowing for mobile phone antennas at 28 GHz and at 60 GHz [data set]. zenodo. http://doi.org/10.5281/zenodo.3249975," .., 2019.

[20] V. Degli-Esposti, F. Fuschini, E. M. Vitucci, and G. Falciasecca, "Measurement and modelling of scattering from buildings," *IEEE Transactions on Antennas and Propagation*, vol. 55, no. 1, pp. 143 – 153, 2007.

[21] "Spatial channel model for multiple input multiple output (MIMO) simulations," *3rd Generation Partnership Project,Sophia Antipolis Cedex,France, Tech. Rep. TR 25.996,*, Sep. 2003.